Journal of Alloys and Compounds 509 (2011) 8937–8943

Contents lists available at ScienceDirect

Journal of Alloys and Compounds

journal homepage: www.elsevier.com/locate/jallcom

Correlation between nanostructural and electrical properties of barium titanate-based glass–ceramic nano-composites

M.S. Al-Assiri [a], M.M. El-Desoky [a,b,*]

[a] Department of Physics, King Khaled University, P.O. Box 9003, Abha, Saudi Arabia
[b] Department of Physics, Faculty of Science, Suez Canal University, Suez, Egypt

ARTICLE INFO

Article history:
Received 20 May 2011
Received in revised form 15 June 2011
Accepted 16 June 2011
Available online 30 June 2011

Keywords:
DSC
TEM
XRD
Density
SPH
Dc conductivity
Barium titanate
Glass–ceramic nanocrystals
Glasses
Dielectric constant

ABSTRACT

Glasses in the system $BaTiO_3$–V_2O_5–Bi_2O_3 have been transformed into glass–ceramic nano-composites by annealing at crystallization temperature T_{cr} determined from DSC thermograms. After annealing they consist of small crystallites embedded in glassy matrix. The crystallization temperature T_{cr} increases with increasing $BaTiO_3$ content. XRD and TEM of the glass–ceramic nano-composites show that nanocrystals were embedded in the glassy matrix with an average grain size of 25 nm. The resulting materials exhibit much higher electrical conductivity than the initial glasses. It was postulated that the major role in the conductivity enhancement of these nanomaterials is played by the developed interfacial regions between crystalline and amorphous phases, in which the concentration of V^{4+}–V^{5+} pairs responsible for electron hopping, has higher than values that inside the glassy matrix. The experimental results were discussed in terms of a model proposed in this work and based on a "core–shell" concept. From the best fits, reasonable values of various small polaron hopping (SPH) parameters were obtained. The conduction was attributed to non-adiabatic hopping of small polaron.

© 2011 Elsevier B.V. All rights reserved.

1. Introduction

Glass–ceramic materials with the size of crystallites smaller than 100 nm (nanocrystallites) are still transparent like glass, and on the other hand, show unique properties. These materials, the so-called glass–ceramic nano-composites, can be obtained by way of nanocrystallization of glasses [1,2]. It is necessary to investigate those properties to understand physical phenomena in these materials and to have better device performance. The glass ceramic nano-composites can be formed with a large diversity of crystal types and crystal sizes (nano, micro etc.). Crystal and grain sizes are the most significant structural parameters in electronic nanocrystalline glassy phases. The preparation of numerous materials by nanocrystallization of glass has been described in the literature [3–9]. This preparation method is simple, cheap and potentially suitable for multifunctional devices [10–17].

Glasses and glass–ceramic nano-composites in system containing V_2O_5 belong to the best electronic conductors [18,4,19–21]. They inherit some structural features and transport properties from the nanocrystalline forms of V_2O_5 and in particular of its α-phase, being often cited as a model of an electronic conductor [21]. On the other hand, in recent years it has been established that the presence of fine grains of foreign phases distributed in moderately conducting matrices (glasses, but also polymer electrolytes or polycrystalline materials) can significantly improve their conductivity [18,4,19,20].

Owing to their semiconducting properties, oxide glasses and corresponding glass–ceramics nano-composites containing large amounts of transition metal oxides (TMO) show interesting electrical properties [23–29]. This behavior is strongly influenced by the simultaneous presence in the glass network of transition metal ion in two different valence states, due to redox processes accruing in the melt at high temperatures in course of preparation. In the conduction of V_2O_5 containing glasses changes, $V^{4+} \rightarrow V^{5+} + e$ takes place between two vanadium ions in glass. The charge transfer is usually termed' small polaron hopping (SPH) [30,31]. The electrical conductivity for such glasses depends strongly upon the local interaction of an electron with its surroundings and distance between vanadium ions [4,19–21].

In our recent work [5], nanostructural, ferroelectric behavior and electrical properties of $BaTiO_3$–V_2O_5 glasses and their nanocrystalline glass–ceramics were studied. Transmission elec-

* Corresponding author at: Department of Physics, King Khaled University, P.O. Box 9003, Abha, Saudi Arabia. Tel.: +20 623666249; fax: +20 623666247.
E-mail addresses: msassiri@kku.edu.sa (M.S. Al-Assiri), mmdesoky@gmail.com (M.M. El-Desoky).

0925-8388/$ – see front matter © 2011 Elsevier B.V. All rights reserved.
doi:10.1016/j.jallcom.2011.06.079

tron micrograph (TEM) and X-ray diffraction (XRD) of nanocrystalline glass ceramics of these samples were indicated nanocrystals with a particle size of 20–30 nm. Also, it was observed that the conductivity of the nanocrystalline glass–ceramics is higher than that of the corresponding glassy phase. The high conductivity of these nanocrystalline glass–ceramics was considered to be due to the presence of nanocrystals. This is attributed to formation of extensive and dense network of electronic conduction paths which were situated between V_2O_5 nanocrystals and on their surface.

The main objective of the corresponding present work is to investigate three subjects $BaTiO_3$–V_2O_5–Bi_2O_3 glasses. The first is to prepare these glasses and glass–ceramic nano-composites. The second is to investigate the compositional dependence of the nanostructural and transport properties of V_2O_5 based glass and corresponding glass–ceramic nano-composites in view of Mott's SPH model [31,32]. The third is to clarify the mechanism of electrical conduction of $BaTiO_3$–V_2O_5–Bi_2O_3 glass and corresponding glass–ceramic nano-composites.

2. Experimental technique

2.1. Sample preparation

Reagent grade $BaTiO_3$ (99.99%), V_2O_5 (99.99%) and Bi_2O_3 (99.999%) were used as raw materials. After mixing in air a batch 12 g with prescribed compositions, the mixture were melted in the temperature range 1000–1100 °C depending on the compositions for one hour. The melt was then poured on a thick copper block and immediately quenched by pressing with another similar copper block. Following this procedure we obtained bulk glass of 2 cm × 2 cm size and about 1 mm in thickness. The glass–ceramics nanocrystals composite were prepared by crystallization the above-mentioned glasses by heating in air at crystallization temperature T_c for eight hours.

2.2. Sample characterizations

The regime of glassy specimens crystallization will be selected on the bases of DSC analysis using Shimatzou differential scanning calorimeter (DSC) 50 instrument. High-resolution transmission electron microscope (JEOL 200 CX) was employed to examine the amorphous/crystalline states of the powders of the heat-treated glass ceramic nano-composites composition. This is also done by X-ray diffractometry (Shimatzou XRD-6000). Selected-area electron diffraction (SAED) studies were carried out on the heat-treated glass ceramic nanocrystals composition to estimate the lattice parameters of the crystalline phase embedded in the glass matrix. The densities of the samples were measured by Archimedes principle using toluene as an immersion liquid. The concentration of vanadium ions, N (cm^{-3}) was estimated using $N = dpN_A/(A_w \times 100)$, where d is the density of the sample, p the weight percentage of atoms, N_A the Avogadro constant and A_w the atomic weight.

2.3. Set up of electrical experiment

The dc conductivity (σ) of the present system was measured at temperatures between room temperature and 473 K. A special measuring cell and furnace are designed and made, which are capable to reach a temperatures as high as 500 °C. Silver paste electrodes deposited on both faces of the polished samples. A multimeter type Keithely 760 was used to collect the dc data. The I–V characteristic between electrodes was confirmed.

3. Results and discussion

3.1. Structural behavior

3.1.1. DSC

Fig. 1 shows differential scanning calorimeter (DSC) thermogram for $15BaTiO_3$–$65V_2O_5$–$20Bi_2O_3$ glass and the composition dependence of glass transition temperature (T_g), crystallization temperature (T_{cr}) melting temperature (T_m) and temperature difference $\Delta T = T_{cr} - T_g$ respectively, for the present glass system. The exothermic peak in the temperature range 347–357 °C corresponds to the crystallization and the peak positions are defined as crystallization peak temperature of T_{cr}. The endothermic dip corresponding to the glass transition (T_g) are observed at 270–305 °C. Also, the endothermic dip due melting temperature

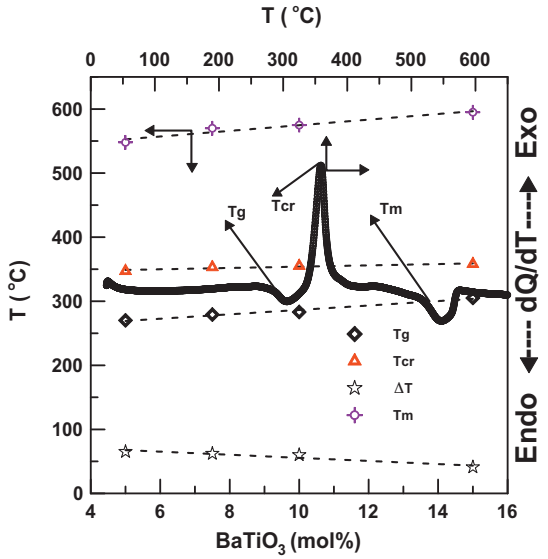

Fig. 1. DSC thermogram for $15BaTiO_3$–$65V_2O_5$–$20Bi_2O_3$ glass and composition dependence of glass transition temperature (T_g), crystallization temperature (T_{cr}) and melting temperature (T_m) temperature difference (ΔT) for different glass compositions.

(T_m) is observed at 548–595 °C. The glass transition temperature T_g increases with increasing $BaTiO_3$ content, suggesting that the present glass system decreases the contribution from the non-bridging oxygen (NBO). It is found that the crystallization temperature (T_{cr}) increases almost linearly with increase in $BaTiO_3$ content [5]. On the other hand, DSC studies [29] on the structure of many glasses have already showed that T_g shows an obvious correlation with the change in the coordination number of the network former and the construction of NBO atoms, which means destruction of the network structure [25]. Generally, T_g shows a distinct increase when the coordination number of the network former increases. Converse to this, a construction of NBO causes a decrease into the T_g. The continuous increase in the T_g in the present system, therefore, seems to suggest continuing decrease in the coordination number of V^{5+} and V^{4+} ions and destruction of NBO atoms [25]. Also, the increase in T_g suggests that the strength of the chemical bond between metal and oxygen atoms becomes strong. This is ascribed to the decreased interatomic distances between metal and oxygen ions leading to decrease in the density [25].

On the other hand, the thermal stability factor, $\Delta T = T_{cr} - T_g$ is also included in Fig. 1.The difference between T_g and T_{cr} is about 65 °C and it decreases with the increase of $BaTiO_3$ content in the glasses indicating that the thermal stability of the glasses decreases with $BaTiO_3$ content. The stability of the glasses could also be predicted by the factor T_g/T_m, i.e., the ratio of the glass transition and melting temperature. For very stable glass the ideal value of T_g/T_m is 0.67 [33]. The T_g/T_m values for all the compositions studied in present system fall in the range 0.49–0.51, being near to that of the ideal value.

3.1.2. XRD

Fig. 2 shows a representative X-ray diffraction patterns (XRD) of the $15BaTiO_3$–$65V_2O_5$–$20Bi_2O_3$ glass (a) and corresponding glass–ceramic nano-composites (b). In case of as-received samples, there is only a wide halo observed with no indication of diffraction peaks. This confirms the amorphous state of initial glasses. A pattern shown Fig. 2(b) was collected for sample after its annealing at crystallization temperature determined from DSC studies. It contains a number of peaks corresponding to a nanocrystalline phases superimposed on a wide halo indicating that there

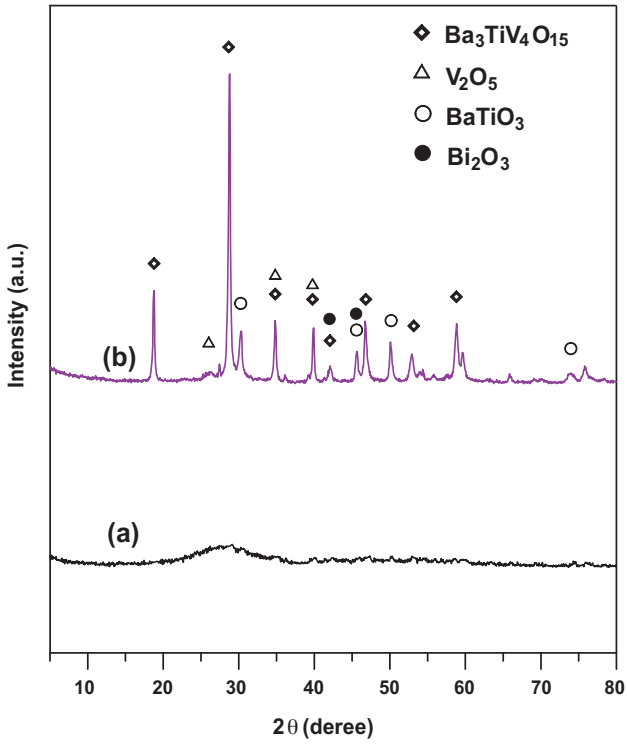

Fig. 2. X-ray diffraction for (a)15$BaTiO_3$–20Bi_2O_3–65V_2O_5 glass and (b) corresponding glass–ceramic nano-composites.

is still substantial amount of amorphous phase. The XRD pattern in the heat-treated sample is a clear indication that annealing at temperature T_{cr} only starts to produce small nanocrystallites in the glass matrix [19–21]. This is a valuable hint, since it means that by adjusting the temperature of annealing, one can control the amount of nanocrystalline grains formed in the material and thus enhance its electrical conductivity (see in Section 3.2). The nanocrystalline phases were recognized as $Ba_3TiV_4O_{15}$, $BaTiO_3$, V_2O_5 and Bi_2O_3. Additionally, there are some new peaks corresponding to the phase which we have not identified yet. Average size of nanocrystallites was predictable from the widths of diffraction peaks, using the Scherrer formula, to ca. 25 nm [19–21]. This is in accordance with the TEM studies that show nearly uniform but slightly agglomerated particles having a grain size of 20–30 nm (Fig. 3(b)).

3.1.3. TEM

The transmission electron micrograph (TEM) along with the selective area electron diffraction pattern (SAED) of the as-quenched 15$BaTiO_3$–65V_2O_5–20Bi_2O_3 glass ample is shown in Fig. 3(a). The SAED pattern that is shown as an inset confirms the amorphous state. However, sharp haloes in this pattern suggest the presence of some amount of crystallinity that is associated with the sample. The electron micrograph, recorded for the sample heat-treated at crystallization temperature for 8 h (Fig. 3(b)) suggests the presence of nearly spherical crystallites of fairly uniform size laying in the range 15–25 nm, evenly dispersed in a glass matrix. The SAED pattern (inset of Fig. 3(b)) and the lattice spacings 'd' obtained therein confirm the presence of $Ba_3TiV_4O_{15}$ and V_2O_5 nanocrystallites. The SAED pattern (inset of Fig. 3(b)) recorded from this sample show a glassy halo but this may be attributed to the strong diffraction of glassy matrix masking the diffraction from crystalline nuclei [5].

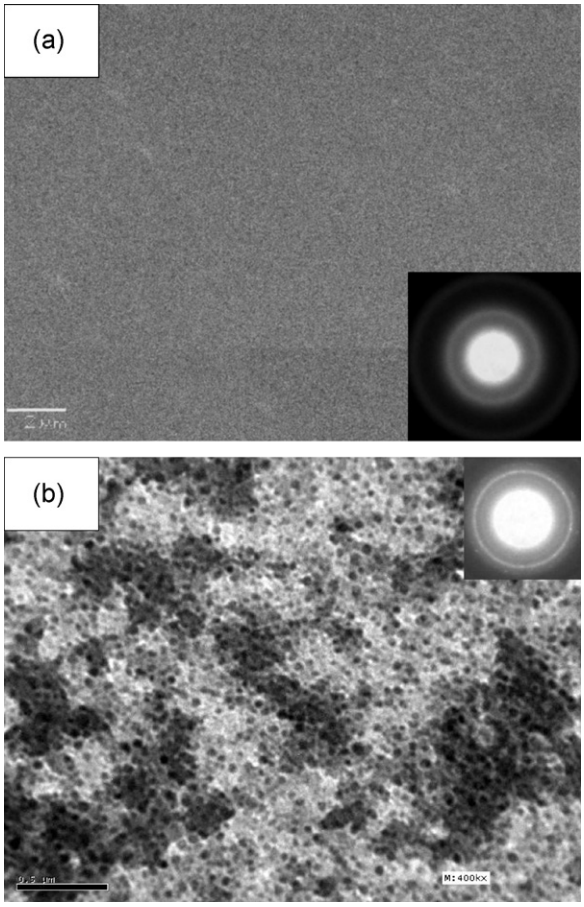

Fig. 3. Transmission electron micrograph (TEM) and selective area electron diffraction (inset) for15$BaTiO_3$–20Bi_2O_3–65V_2O_5 (a) glass and (b) corresponding glass–ceramic nano-composites.

3.1.4. Density

The density, *d*, for the glasses and corresponding glass–ceramic nano-composites are shown in Fig. 4. These properties changed linearly as a function of glasses and corresponding glass–ceramic nano-composites. It is observed that the density increases gradu-

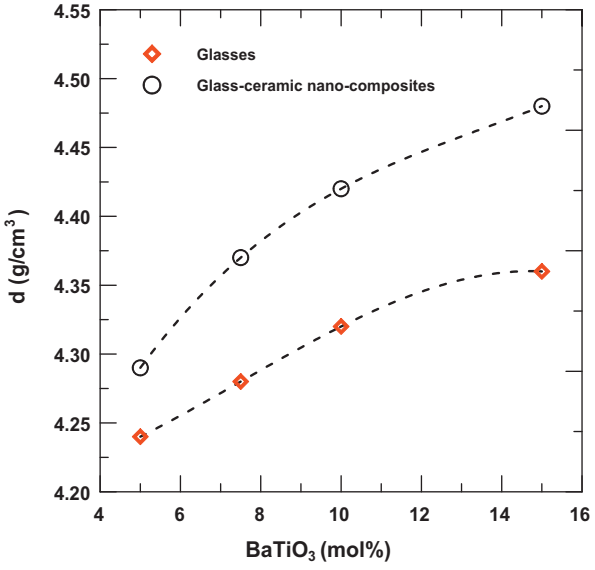

Fig. 4. Composition dependence of density (d) for $BaTiO_3$–V_2O_5–Bi_2O_3 glasses and corresponding glass–ceramic nano-composites.

Table 1
Some important physical properties and SPH parameters of $BaTiO_3$–V_2O_5–Bi_2O_3 glasses.

Nominal composition (mol%)			d ±0.02 (g cm^{-3})	W_{glass} ±0.01 (eV)	R ±0.01 (nm)	N ±0.01 ($\times10^{22}$ cm^{-3})	r_p ±0.001 (nm)	θ_D ±1 (K)	ν_o ±0.01 ($\times10^{13}$ Hz)	$N(E_F)$ ($\times10^{21}$) (eV^{-1} cm^{-3})
$BaTiO_3$	V_2O_5	Bi_2O_3								
5	75	20	4.24	0.38	0.454	1.064	0.183	833	1.74	6.72
7.5	72.5	20	4.28	0.44	0.452	1.079	0.182	810	1.70	5.88
10	70	20	4.32	0.46	0.451	1.089	0.181	775	1.55	5.66
15	65	20	4.36	0.50	0.449	1.098	0.180	743	1.48	5.28

Table 2
Some important physical properties and SPH parameters of $BaTiO_3$–V_2O_5–Bi_2O_3 glass–ceramic nanocrystals.

Nominal composition (mol%)			d ±0.02 (g cm^{-3})	W_{nano} ±0.01 (eV)	R ±0.01 (nm)	N ±0.01 ($\times10^{22}$ cm^{-3})	r_p ±0.001 (nm)	θ_D ±1 (K)	ν_o ±0.01 ($\times10^{13}$ Hz)	$N(E_F)$ ($\times10^{21}$) (eV^{-1} cm^{-3})
$BaTiO_3$	V_2O_5	Bi_2O_3								
5	75	20	4.29	0.13	0.452	1.08	0.182	645	1.29	19.89
7.5	72.5	20	4.37	0.17	0.450	1.10	0.180	666	1.33	15.41
10	70	20	4.42	0.20	0.447	1.12	0.179	689	1.37	13.37
15	65	20	4.48	0.22	0.445	1.13	0.178	714	1.43	12.32

ally with the increase of $BaTiO_3$ content. The density results show that as Ti cation concentration increases the glasses and corresponding glass–ceramic nano-composites structure becomes less open, allowing for the probable formation of decreasing number of NBO [29]. In this present system the densities vary from 4.24 up to 4.36 g/cm^3 and 4.29 up to 4.48 g/cm^3 for glasses and corresponding glass–ceramic nano-composites, respectively (Tables 1 and 2).

3.2. DC conductivity

3.2.1. Conductivity and activation energy

The logarithmic dc conductivity, σ, as a function of reciprocal temperature of the present glasses and corresponding glass–ceramic nano-composites are shown in Fig. 5(a) and (b). It is observed from the figure linear temperature dependence up to a temperature $\theta_D/2$ (θ_D Debye temperature). Such behavior is typical for the hopping of electrons or polarons between mixed valence states [18,4,19–22]. So the experimental conductivity data above $\theta_D/2$ were fitted with SPH model proposed by Mott [30,31]. The high temperature activation energy was computed from the slope of each curve in the highest range of the temperature measured. The experimental conductivity data in such a situation is well described by activation energy for conduction given by Mott formula [30,31].

$$\sigma = \sigma_0 \exp\left(\frac{-W}{kT}\right) \quad (1)$$

where σ_0 is a pre-exponential factor, W is the activation energy and k is the Boltzmann constant. The variation of the high temperature conductivity and the high temperature activation energy of glasses and corresponding glass–ceramic nano-composites with composition are shown in Fig. 6. It is clear from the figure that the conductivity decreases while the activation energy increases with the increase of the $BaTiO_3$ content. Such a behavior is a feature of SPH [25,26]. The high value of activation energy and low value of electrical conductivity are similar to those for $SrTiO_3$–V_2O_5–PbO_2 and $BaTiO_5$–V_2O_3 glasses [3,5]. This change in conductivity and activation energy may help to detect the structural changes as a consequence of increasing $BaTiO_3$ and decreasing V_2O_5 content.

Fig. 6 presents variation in conductivity with $BaTiO_3$ content at a fixed temperature (400 K) of glasses and corresponding glass–ceramic nano-composites. It is interesting to note that these corresponding glass–ceramic nano-composites show high conductivity compared to the samples in glassy phase [3,5]. The enhancement of conductivity of these corresponding glass–ceramic nano-composites is considered to be due to the presence of nanocrystals with an average grain size of 20–30 nm as reported in TEM and XRD results. Such remarkable increases in conductivity have been reported in other $SrTiO_3$–V_2O_5–PbO_2 and $BaTiO_5$–V_2O_3 glasses [3,5]. With an increase in conductivity by nanocrystallization, the activation energies for conduction were found to be W_{nano} = 0.13–0.22 eV at high temperatures which are much lower than those for the as-received glasses W_{glass} = 0.50–0.38 eV at high temperatures (Tables 1 and 2). This means a increase of V^{4+} ion ratio causing the activation energy, W, to decrease and σ to increase (Fig. 6). In the $BaTiO_3$–V_2O_5–Bi_2O_3 system of our present investigation, the $BaTiO_3$ addition decreased the conductivity (Fig. 5). Generally, it is known that the addition of $BaTiO_3$ to glass decreases the conductivity as a result of decreasing non-bridging oxygen (NBO) cations [3,5]. This may decrease the open structure, through which the charge carriers can move with lower mobility. This result is consistent with density results (as shown in Fig. 4).

On the other hand, the improvement of electrical conductivity of glass–ceramic nano-composites system under study can be explained in the following way. The most important for electronic conduction in the glasses of the $BaTiO_3$–V_2O_5–Bi_2O_3 system with high amount of V_2O_5 is the spatial distribution of V^{4+} and V^{5+} ions which are centers of hopping for electrons [3,4,19–21]. In the initial glass, there is a random distribution of such centers. The annealing at temperatures close to crystallization temperature leads to formation of nanocrystallites of V_2O_5 embedded in the glass matrix. Since the average size of these grains is small about 20–30 nm, the interface between crystalline and amorphous phases is very extensively ramified and strongly influences overall electrical properties of the nanomaterial as reported in TEM and XRD. In particular, it may contain the improved concentration of V^{4+} and V^{5+} centers dispersed on the surface of V_2O_5 crystallites [3,4,19–21]. However, This enhancement of electrical conductivity can be attributed to (i) an increasing of concentration of V^{4+}–V^{5+} pairs (a possible reason of this increase between surfaces of nanocrystallites and glassy phase) and (ii) formation of defective, well-conducting regions along the glass-crystallites interfaces [3,4,19–21].

In addition, the decrease in dc conductivity and the increase in activation energy for the present samples suggest some changes in conduction mechanisms. It has been previously reported [24–29] that in glasses containing vanadium oxide the dc conductivity is electronic and depends strongly upon the average distance, R,

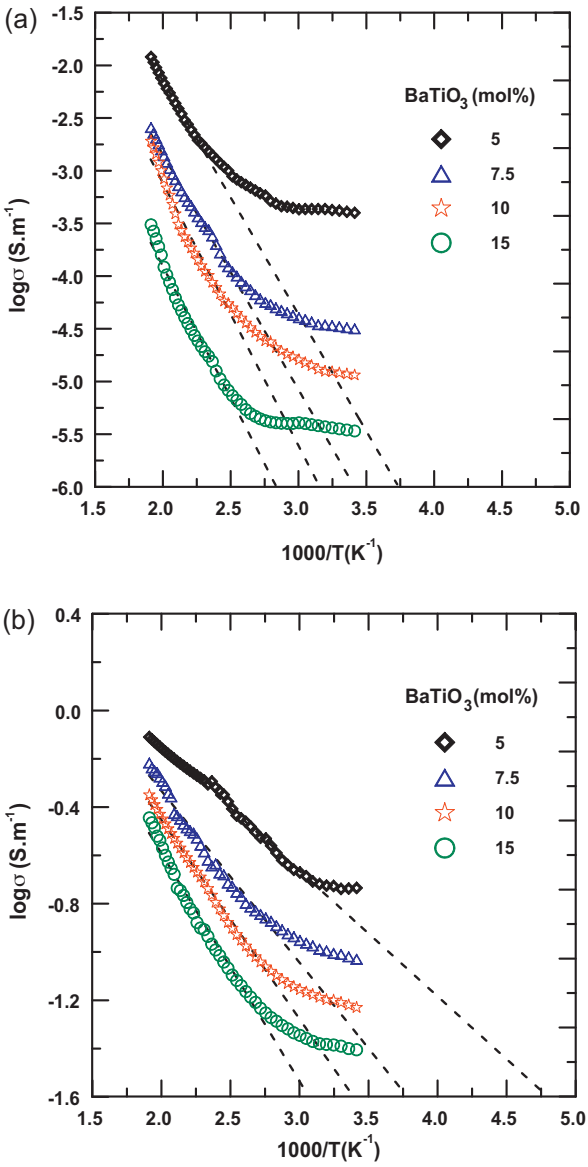

Fig. 5. Temperature dependence of dc conductivity (σ) as a function of $BaTiO_3$ content for (a) glasses and (b) corresponding glass–ceramic nano-composites.

between the vanadium ions. The average distance, R, was calculated for the present system (see Tables 1 and 2) from the relation $R = (1/N)^{1/3}$, where N is the concentration of vanadium ions per unit volume, calculated from batch composition and the measured density. The density, d, the concentration of vanadium ions per unit volume, N, and average distance, R, are given in Tables 1 and 2 for the glasses and corresponding glass–ceramic nano-composites system, respectively. The relation between the average distance, R, and activation energy, W, for glasses and corresponding glass–ceramic nano-composites is illustrated in Fig. 7. These results agree with the results suggested by El-Desoky [3,5] described the dependence of W on the V–O–V site distance.

On the other hand, the theoretical expression for that energy includes a term $W = W_0(1 - r_p/R)$, where W_0 is constant and r_p denotes a radius of small polaron [30,31]. All above formulas indicate that electronic conductivity increases and activation energy decreases when the distance R between hopping centers decreases. In our case one can expect that due to nanocrystallization process the concentration of V^{4+}–V^{5+}pairs is higher near the surfaces of the newly formed crystallites than in the remaining glassy phase

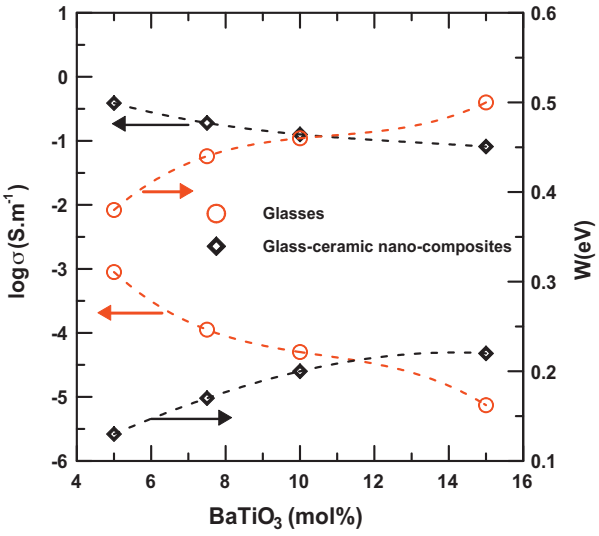

Fig. 6. The relation between conductivity and activation energy as a function of $BaTiO_3$ content for glasses and glass–ceramic nano-composites.

and inside the crystallites. It is widely known that many important characteristics of nanomaterials originate from the defective nature of the interfaces between crystalline and amorphous phases [3,4]. Higher concentration of V^{4+}–V^{5+} pairs leads to smaller average distance between the hopping centers, and according to Mott model [30,31] it causes an increase in conductivity. The interface regions of higher than average conductivity form a kind of "easy conduction paths" for electrons [3,4,19–21].

Pietrzak et al. [19] have reported model for explain the conductivity improvement caused by nanocrystallization. However in the present case, from the TEM and conductivity data, it is more likely that a crystalline part of the grain (sense by XRD) is enveloped by a strongly distorted or even amorphous one. The whole grain, with its crystalline inner part and distorted outer part is seen in TEM micrographs. This description is in line with a "core–shell" model of the nanosized grains in thermally nanocrystallized materials such as the one under study. According to this model a grain consists of an inner fully crystalline "core" and an outer highly dis-

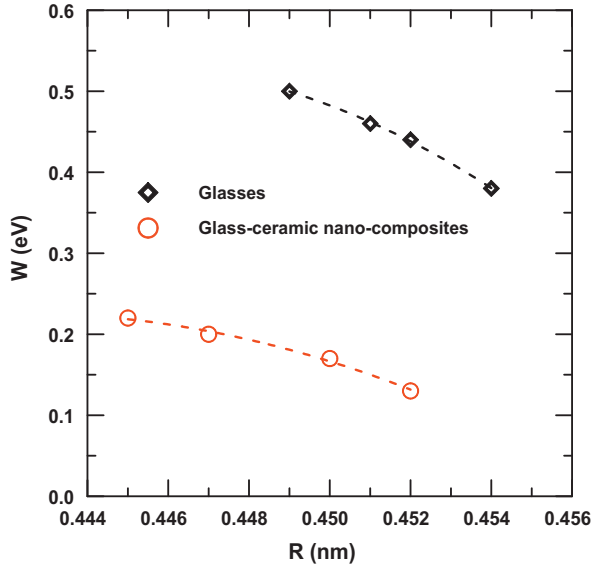

Fig. 7. Effect of average distance (R) on activation energy (W) for different glasses and glass–ceramic nano-composites.

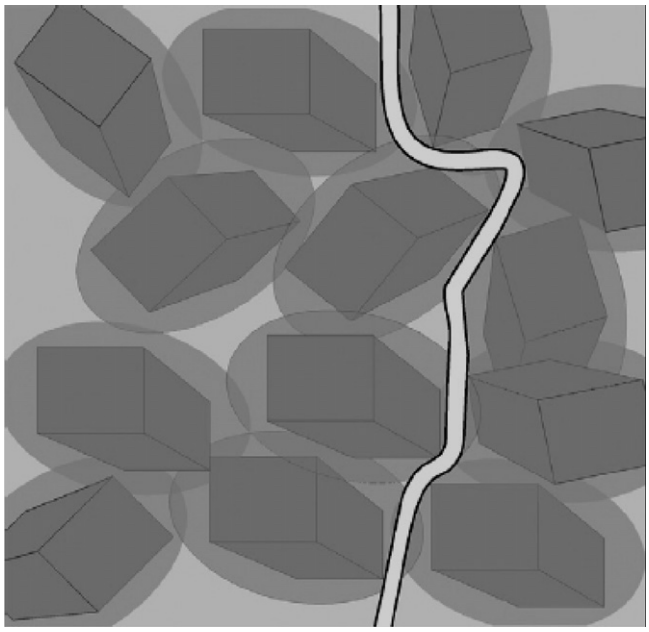

Fig. 8. A model of the easy conduction paths in studied nanomaterials using a "core–shell" concept Ref. [19].

ordered, defective and non-stoichiometric "shell" [19]. The same "core–shell" concept can explain the conductivity improvement caused by nanocrystallization. Fig. 8 shows a representation of such a model. The overlapping and intersecting defective shells around crystalline cores can form a complicated system of paths for facilitated electron transport. The mechanism of electronic transport in vanadium oxides consists in SPH between aliovalent V^{4+} and V^{5+} sites. In the regions where the local concentration of the V^{4+}–V^{5+} pairs is high, the conductivity is also high. Such a circumstance takes place inside and around the defective grain-shell areas. This significant improvement of electrical conductivity after nanocrystallization is attributed to formation of extensive and dense network of electronic conduction paths which are situated between vanadium nanocrystals and on their surface [3,4,19–21].

3.2.2. Conduction mechanism

Mott [30] proposed a model for conduction processes in the transition metal oxides (TMO) glasses. In this model, the conduction process is considered in terms of phonon assisted hopping of small polarons between localized states. The dc conductivity in the Mott model for the nearest neighbours hopping in non-adiabatic regime at high temperatures $T > \theta_D/2$ is given by: [31]

$$\sigma = \frac{\nu_o N e^2 R^2}{kT} C(1-C)\exp(-2\alpha R)\exp\left(\frac{-W}{kT}\right) = \sigma_0 \exp\left(\frac{-W}{kT}\right) \quad (2)$$

The pre-exponential factor (σ_0) in Eq. (2) is given by

$$\sigma_0 = \frac{\nu_o N e^2 R^2}{kT} C(1-C)\exp(-2\alpha R) \quad (3)$$

where ν_o is the optical phonon frequency, α is the tunnelling factor (the ratio of wave function decay), N the transition metal density, C the fraction of reduced transition metal ion and W is the activation energy for hopping conduction. Assuming a strong electron–phonon interaction, Austin and Mott [30,31] have shown that

$$W = W_H + \frac{W_D}{2} \quad \text{for } T > \frac{\theta_D}{2} \quad (4a)$$

$$W = W_D \quad \text{for } T < \frac{\theta_D}{4} \quad (4b)$$

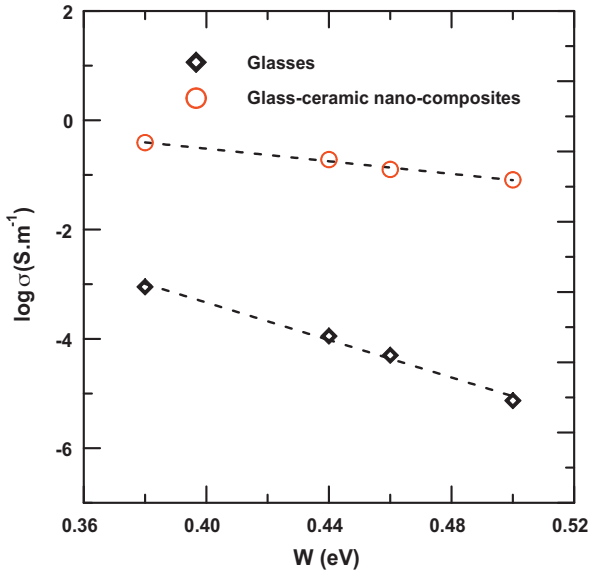

Fig. 9. Effect of activation energy (W) on dc conductivity (σ) at $T = 400$ K for different glasses and glass–ceramic nano-composites.

where W_H is the polaron hopping energy, and an energy difference W_D which might exist between the initial and final sites due to variation in the local arrangements of ions.

The nature of polaron hopping mechanism (adiabatic or non-adiabatic), of all these glasses and corresponding glass–ceramic nano-composites can be estimated from a plot of logarithm of the conductivity against activation energy (Fig. 9) at fixed experimental temperature T [24–29]. It is expected that the hopping will be in the adiabatic regime if the temperature estimated T_e, from the slope of such a plot, is close to the experimental temperature T. Otherwise the hopping will be in the non-adiabatic regime. From the plot of $\ln\sigma$ against W at $T = 400$ K as shown in Fig. 10, the experimental slopes were not equal to the theoretical slopes. The estimated temperature (T_e) calculated from the experimental slopes were $T_e = 286$ K, and 875 K for glasses and corresponding glass–ceramic nano-composites, respectively, which were larger than that of the

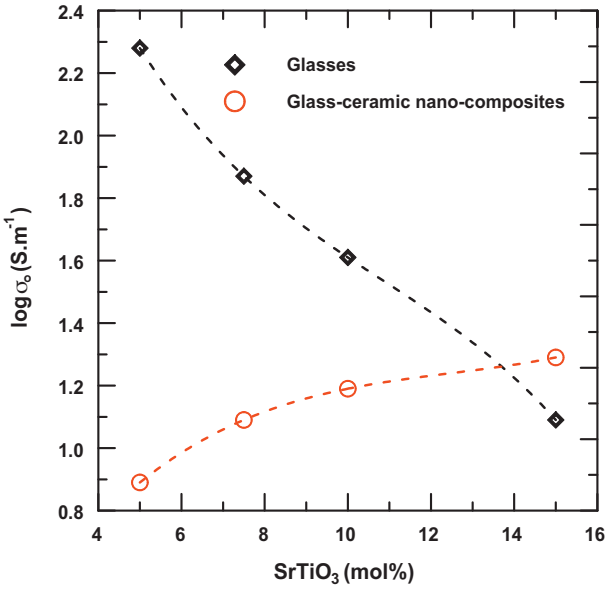

Fig. 10. Effect of $BaTiO_3$ content on pre-exponential factor (σ_o) for different glasses and glass–ceramic nano-composites.

experimental temperature (T = 400 K). Fig. 10 presents the effect of $BaTiO_3$ content on the pre-exponential factors (σ_0) obtained from the least squares straight line fits of the data indicating an independent in σ_0 with $BaTiO_3$content from 5 to 15 mol%. For both results, it can be concluded that the conduction mechanism in the present glasses and corresponding glass–ceramic nano-composites is due to the non-adiabatic hopping of the polarons [24–29].

3.2.3. Polaron hopping parameters

Holstein [32] suggests a method for calculating the polaron hopping energy W_H as;

$$W_H = \tfrac{1}{4} N \sum_p [\gamma_p]^2 \hbar\omega_p \quad (5)$$

where $[\gamma_p]^2$ is the electron–phonon coupling constant and ω_p is the optical phonons frequency. On the other hand, Bogomolov et al. [33] have calculated the polaron radius, r_p, for a non-dispersive system of frequency υ_o for Eq. (5) as;

$$r_p = \left(\frac{\pi}{6}\right)^{1/3} \frac{R}{2} \quad (6)$$

The values of the polaron radii calculated from Eq. (6), using R from Tables 1 and 2 are shown in the same two tables for the present system. Although the possible effect of disorder has been neglected in the above calculation, the small values of polaron radii suggest that the polarons are highly localized.

The density of states for thermally activated electron hopping near the Fermi level from basic principles is given as [3,31].

$$N(E_F) = \frac{3}{4\pi R^3 W} \quad (7)$$

The results for the glasses and corresponding glass–ceramic nano-composites are listed in Tables 1 and 2. The values of $N(E_F)$ are reasonable for localized states [24–29].

We estimated the optical phonon frequency, (ν_o) in Eq. (3) using the experimental data from Tables 1 and 2, according to $k\theta_D = h\nu_o$ (h is the Plank's constant). To determine ν_o for the different compositions, the Debye temperature θ_D was estimated by $T > \theta_D/2$ using the θ_D values given in Tables 1 and 2 at the point of significant change of the slope of the curves shown in Fig. 5(a) and (b). θ_D of the present system was obtained to be 743–833 K and 645–714 K for glasses and corresponding glass–ceramic nano-composites, respectively. These values are similar to those values of $BaTiO_3$–V_2O_5 and $SrTiO_3$–V_2O_5–PbO_2 glasses [3,5]. Thus, these estimated θ_D values are considered to be physically reasonable. Then, using θ_D value, ν_o was calculated. The values of θ_D and ν_o are summarized in Tables 1 and 2.

4. Conclusion

Novel glass–ceramic nano-composites based on $BaTiO_3$–V_2O_5–Bi_2O_3 glasses were prepared via annealing at crystallization temperature T_{cr} determined from DSC thermograms. The nanostructural and electrical properties were investigated by DSC, TEM, XRD, density, and dc conductivity, respectively. Using a combination of these methods, it was possible to find correlation between nanostructural and electrical properties of the obtained nonamaterial and to optimize conditions of its synthesis. It was found out that the electronic conductivity of the original glasses can be considerably enhanced by appropriate nanocrystallization at temperatures close to beginning of T_{cr}. Increase in conductivity arises from the modification of the nanostructural. It was shown by XRD and TEM studies that by appropriate heat-treatment glasses can be turned into nanomaterials consisting of crystallites with an average size 25 nm embedded in the glassy matrix. The resulting materials exhibit much higher electrical conductivity than the initial glasses. The major role in the conductivity enhancement of these nanomaterials is played by the developed interfacial regions between nanocrystalline and glassy phases, in which the concentration of V^{4+}–V^{5+}, pairs responsible for electron hopping in present system, is higher than inside the glassy matrix and the formed nanocrystallites. The experimental results were discussed in terms of a model proposed in this work and based on a "core–shell" concept. From the best fits, reasonable values of various small polaron hopping (SPH) parameters were obtained.

Acknowledgment

The authors thank KAST of Saudi Arabia, for financial support (grant no. 08-NAN146-7)

References

[1] M. Eroda, I. Wacawska, L. Stoch, M. Reben, J. Therm. Anal. Calorim. 77 (2004) 193.
[2] X.L. Duan, D.R. Yuan, F.P. Yu, L.H. Wang, Appl. Phys. Lett. 89 (2006) 183119.
[3] M.M. El-Desoky, H.S.S. Zayed, F.A. Ibrahim, H.S. Ragab, Physica B 404 (2009) 4125.
[4] M.M. El-Desoky, Mater. Chem. Phys. 119 (2010) 389.
[5] J.E. Garbarczyk, M. Wasiucionek, P. Jozwiak, J.L. Nowinski, C.M. Julien, Solid State Ionics 180 (2009) 531.
[6] J.E. Garbarczyk, P. Jozwiak, M. Wasiucionek, J.L. Nowinski, Solid State Ionics 175 (2004) 691.
[7] J.E. Garbarczyk, P. Jozwiak, M. Wasiucionek, J.L. Nowinski, Solid State Ionics 177 (2006) 2585.
[8] M.Y. Hassaana, F.M. Ebrahima, A.G. Mostafa, M.M. El-Desoky, Mater. Chem. Phys. 129 (2011) 380.
[9] M. Foltyn, M. Wasiucionek, J.E. Garbarczyk, J.L. Nowinski, Solid State Ionics 176 (2005) 2137.
[10] Y. Hu, C.L. Huang, J. Non-Cryst. Solids 278 (2000) 170.
[11] N.S. Prasad, K.B.R. Varma, J. Non-Cryst. Solids 351 (2005) 1455.
[12] N.S. Prasad, K.B.R. Varma, Y. Takahashi, Y. Benino, T. Fujiwara, T. Komatsu, J. Solid State Chem. 173 (2003) 209.
[13] M. Sadhukhan, D.K. Modak, B.K. Chaudhuri, J. Appl. Phys. 85 (1999) 3477.
[14] P. Prapitpongwanich, R. Harizanova, K. Pengpat, C. Rüssel, Mater. Lett. 63 (2009) 1027.
[15] N.F. Borelli, J. Appl. Phys. 38 (1967) 4243.
[16] K. Tanaka, K. Kashima, N. Soga, A. Mito, H. Nasu, J. Non-Cryst. Solids 185 (1995) 123.
[17] K. Hirao, Bull. Ceram. Soc. Jpn. 38 (5) (2003) 323.
[18] K. Hirao, Bull. Ceram. Soc. Jpn. 36 (9) (2001) 652.
[19] T.K. Pietrzak, J.E. Garbarczyk, I. Gorzkowska, M. Wasiucionek, J.L. Nowinski, S. Gierlotka, P. Jozwiak, J. Power Sources 194 (2009) 73.
[20] J.E. Garbarczyk, P. Jozwiak, M. Wasiucionek, J.L. Nowinski, J. Power Sources 173 (2007) 743.
[21] M.M. El-Desoky, F.A. Ibrahim, A.G. Mostafa, M.Y. Hassaan, Mater. Res. Bull. 45 (2010) 1122.
[22] M.M. El-Desoky, Phys. Status Solidi (a) 195 (2003) 422.
[23] Y. Ohta, M. Kitayama, K. Kaneko, S. Toh, F. Shimiz, K. Morinaga, J. Am. Ceram. Soc. 88 (6) (2005) 1634.
[24] M.M. El-Desoky, A. Al-Shahrani, J. Mater. Sci.: Mater. Electron. 16 (2005) 221.
[25] M.M. El-Desoky, M.S. Al-Assiri, Mater. Sci. Eng. 37 (2007) 237.
[26] A. Al-Hajry, A. Al-Shahrani, M.M. El-Desoky, Mater. Chem. Phys. 95 (2006) 300.
[27] M.M. El-Desoky, A. Al-Shahrani, Physica B 371 (2006) 95.
[28] A. Al-Shahrani, A. Al-Hajry, M.M. El-Desoky, Phys. Status Solidi (a) 300 (2003) 378.
[29] M.S. Al-Assiri, S.A. Salem, M.M. El-Desoky, J. Phys. Chem. Solids 57 (2006) 1873.
[30] N.F. Mott, J. Non-Cryst. Solids 1 (1968) 1.
[31] I.G. Austin, N.F. Mott, Adv. Phys. 18 (1969) 41.
[32] T. Holstein, Ann. Phys. 8 (1959) 343.
[33] V.N. Bogomolov, E.K. Kudinev, U.N. Firsov, Sov. Phys. Solid State 9 (1968) 2502.